Title

Targeted Amino Acid Substitution Overcomes Scale-Up Challenges with the Human C5a-Derived Decapeptide Immunostimulant EP67.

Journal

ACS Infectious Diseases, 6(5)

Authors

Alshammari, Abdulraman

Smith, D

Parriott, Jake

et al.

Publication Date

2020-05-08

DOI

10.1021/acsinfecdis.0c00005

Peer reviewed

HHS Public Access

Author manuscript

ACS Infect Dis. Author manuscript; available in PMC 2020 June 08.

Published in final edited form as:

ACS Infect Dis. 2020 May 08; 6(5): 1169–1181. doi:10.1021/acsinfecdis.0c00005.

Targeted Amino Acid Substitution Overcomes Scale-Up Challenges with the Human C5a-Derived Decapeptide Immunostimulant EP67

Abdulraman M. Alshammari[b], **D. David Smith**[c], **Jake Parriott**[b], **Jason P. Stewart**[b], **Stephen M. Curran**[b], **Russell J. McCulloh**[d], **Peter A. Barry**[e], **Smita S. Iyer**[f], **Nicholas Palermo**[g], **Joy A. Phillips**[h], **Yuxiang Dong**[b], **Donald R. Ronning**[b], **Jonathan L. Vennerstrom**[b], **Sam D. Sanderson**[b], **Joseph A. Vetro**[a,b,*]

[a]Center for Drug Delivery and Nanomedicine, College of Pharmacy, University of Nebraska Medical Center, Omaha, NE 68198-6025, USA

[b]Department of Pharmaceutical Sciences, College of Pharmacy, University of Nebraska Medical Center, Omaha, NE 68198-6025, USA

[c]Department of Biomedical Sciences, Creighton University, 2500 California Plaza, Omaha, NE 68178, USA

[d]Department of Pediatrics, Children's Hospital and Medical Center, Omaha, Nebraska, 68114, USA

[e]Center for Immunology and Infectious Diseases, Pathology and Laboratory Medicine, UC Davis School of Medicine, Davis, CA 95817, USA

[f]Center for Immunology and Infectious Diseases, Pathology, Microbiology & Immunology, UC Davis, School of Veterinary Medicine, California National Primate Research Center, Davis, CA 95817, USA

[g]Holland Computing Center, University of Nebraska-Lincoln, Lincoln, NE 68588, USA

[h]Donald P. Shiley BioScience Center, San Diego State University, San Diego, CA 92115, USA

Abstract

EP67 is a second-generation, human C5a-derived decapeptide agonist of C5a Receptor 1 (C5aR1/CD88) that selectively activates mononuclear phagocytes over neutrophils to potentiate protective innate and adaptive immune responses while potentially minimizing neutrophil-mediated toxicity. Pro^7 and *N*-methyl-Leu^8 ($Me\text{-}Leu^8$) amino acid residues within EP67 likely induce backbone structural changes that increase potency and selective activation of mononuclear phagocytes over neutrophils vs. first-generation EP54. Low coupling efficiency between Pro^7 and $Me\text{-}Leu^8$ and

*Corresponding Author. jvetro@unmc.edu.

AUTHOR INFORMATION: Joseph A. Vetro, PhD, Department of Pharmaceutical Sciences, UNMC College of Pharmacy, 986020 Nebraska Medical Center, LTC 11706, Omaha, NE 68198-6020, USA.

SUPPORTING INFORMATION

This information is available free of charge on the ACS Publications website

CONFLICT OF INTEREST

The authors declare no competing financial interest.

challenging purification by HPLC, however, greatly increase scale-up costs of EP67 for clinical use. Thus, the goal of this study was to determine whether replacing Pro^7 and/or Me-Leu^8 with large-scale amenable amino acid residues predicted to induce similar structural changes (cyclohexylalanine^7 and/or leucine^8) sufficiently preserves EP67 activity in primary human mononuclear phagocytes and neutrophils. We found that, depending on the secreted cytokine and mononuclear phagocyte, EP67 analogs had (i.) similar or lower (29 to 39%) potency and similar, increased (9.5 to 45%), or decreased (5 to 23%) efficacy for IL-6 and TNF-α secretion from mononuclear phagocytes and (ii.) similar potency and similar or decreased (21% to 24%) efficacy for myeloperoxidase secretion from human neutrophils without affecting selective activation of human mononuclear phagocytes. Thus, replacing Pro^7 and/or Me-Leu^8 with large-scale amenable amino acid residues predicted to induce similar structural changes is a suitable strategy to overcome scale-up challenges with EP67.

Table of Contents Graphic

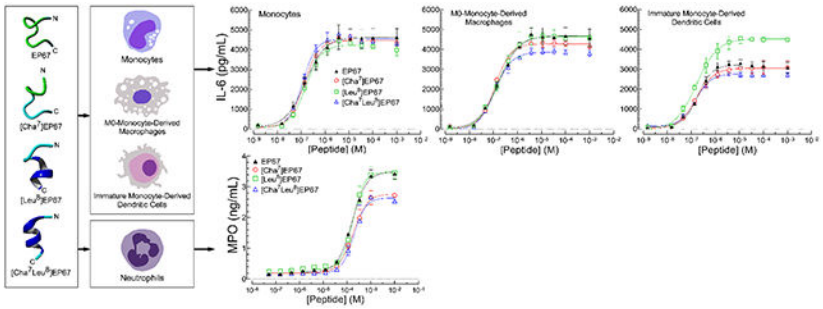

Keywords

host-directed therapy; host-derived immunostimulant; complement peptide-derived immunostimulant (CPDI); mucosal adjuvant; human C5a desArg; EP54

Immunization has eliminated or greatly reduced the incidence of over 30 infectious diseases caused by bacterial and viral pathogens including CRS, diptheria, *Haemophilus influenzae*, hepatitis A, hepatitis B (acute), influenza, measles, mumps, pertussis, pneumococcus (invasive), polio (paralytic), rotavirus, rubella, smallpox, tetanus, and varicella [1–2]. There is also clinical evidence that vaccine administration within a critical period of time after pathogen exposure can minimize or prevent infectious diseases caused by hepatitis A virus, hepatitis B virus, measles virus, mumps virus, varicella zoster virus, rabies virus, and smallpox virus by increasing the rate and magnitude of protective innate and/or adaptive immune responses [3]. Despite this success, licensed vaccines are unavailable (e.g., *S. aureus*, *M. tuberculosis*, *L. monocytogenes*, HIV, CMV, and RSV) or only partially effective (e.g., influenza virus, *B. pertussis*) for at least 35 bacterial and viral pathogens that are suitable targets for vaccine development [2, 4–6]. Furthermore, only a single partially effective licensed vaccine is available for protozoan pathogens (*P. falciparum*) and no licensed vaccines are available for fungal pathogens [7–8].

A key requirement for licensed vaccines is the ability to safely generate long-lived, pathogen-specific adaptive immune responses that reduce, control, and clear pathogen from

the site of infection (i.e., protective adaptive immune responses) above threshold levels that correlate with elimination or significant decrease in the incidence of infectious disease in a given population [9–12]. The majority of licensed vaccines are proposed to prevent infectious disease primarily by generating one or more subsets of long-lived memory B-cells that maintain or quickly establish sufficient levels of neutralizing antibodies against pathogens with surface antigens that do not change over time [13–15]. Many pathogens without licensed vaccines, however, have hypervariable surface antigens, multiple strains, and/or short extracellular phases that additionally require the generation long-lived protective $CD4^+$ and/or $CD8^+$ memory T-cells [16–19].

Vaccines composed of live-attenuated bacterial, fungal, protozoan, or viral pathogens that safely mimic natural infection are the most likely to generate adequate levels of long-lived protective memory B-cells and T-cells against the wild-type pathogen by sufficiently activating macrophages and dendritic cells, prolonging antigen presentation by antigen-presenting cells (APC), and inducing the most appropriate protective adaptive immune responses [18]. Live-Attenuated vaccines, however, are (i.) limited to pathogens that increase protection after natural infection and can be grown in culture, (ii.) are difficult to establish for most bacterial pathogens, (iii.) take a long time to develop, (iv.) are rarely safe and stable, (v.) may not cross-protect against other pathogenic strains, (vi.) are not suitable for pregnant women or immunocompromised patients, and (vii.) may revert to wild-type virulence (e.g., poliovirus) [18, 20–22]. Non-replicating vaccines composed of killed (bacteria) or inactivated (virus) pathogens (Killed-Inactivated vaccines) can potentially overcome the safety issues of Live-Attenuated vaccines but not the remaining limitations [18]. Killed-Inactivated vaccines are also less immunogenic than Live-Attenuated vaccines, provide a shorter duration of protection, and do not generate appreciable levels of $CD8^+$ T-cells. Although precipitating Killed-Inactivated vaccines into micrometer-sized particulates by adsorption to pre-formed aluminum hydroxide or aluminum phosphate particulate gels (alum adjuvant) increases antibody titers, it does not increase the generation of long-lived $CD8^+$ T-cells and may polarize toward Th2 adaptive immune responses that are potentially less effective against bacterial, fungal, viral, and protozoan pathogens [23].

The limitations of Live-Attenuated and Killed-Inactivated vaccines and desire for well-defined vaccines with more predictable activity have led to the development of vaccines composed of one or more immunogens from the pathogen that are targeted by protective antibody and T-cell responses after infection (subunit and recombinant vaccines) [8, 20, 24]. Recombinant vaccines also allow incorporating protein immunogens engineered to generate more potent and broadly protective memory B-cells and T-cells [25]. Subunit and recombinant vaccines, however, require the inclusion of immunostimulant molecules to generate long-lived adaptive immune responses because they lack immunostimulatory molecules from the wild-type pathogen to sufficiently activate macrophages, dendritic cells, and recruited inflammatory monocytes (mononuclear phagocytes) at the vaccine administration site [18]. There is also a growing interest in using immunostimulant molecules to increase the rate and magnitude of protective innate immune responses after pathogen exposure in combination with conventional antimicrobial drugs (adjunct immunotherapy) [26]. As such, numerous immunostimulant molecules are being developed to safely activate mononuclear phagocytes through well-defined signaling pathways [23].

Given their role in the potentiation of innate and adaptive immune responses against bacterial, fungal, protozoan, and viral infections [27–28], the majority of immunostimulant molecules are currently derived from pathogen-associated molecular pattern molecules (PAMPs) that activate mononuclear phagocytes through cell-associated pattern recognition receptors (PRRs) [29–30]. Two PAMP-derived PRR agonists that stimulate PRRs from the Toll-Like Receptor (TLR) family, CpG 1018 (TLR9) and Monophosphoryl Lipid A (TLR4), are also the first immunostimulant molecules to be included alone (CpG 1018) or in combination with other adjuvants (Monophosphoryl Lipid A) in licensed vaccines [31]. The large number of PRRs and differences in adaptive immune responses generated by individual PRRs, however, may complicate identifying individual or combinations of PRR agonists that simultaneously increase the generation of long-lived B-cells, $CD4^+$, and $CD8^+$ T-cells [32].

In contrast to PAMPs, the Complement System is a less exploited but equally important host defense against bacterial, fungal, protozoan, and viral infections [30, 33–34]. Activation of the Complement System by foreign microbes at the site of infection through Classical, Alternative, or Lectin pathways initiates a proteolytic cascade of C proteins that converges on the production of three immunostimulatory complement peptides, C3a, C4a, and C5a (originally described as anaphylatoxins) [35] from inactive C3, C4, and C5, respectively, that are immediately metabolized into less potent des Arg forms lacking C-terminal Arg, and the concurrent formation of membrane attack complexes (MAC) [36]. These products then “complement” host immunity by increasing local and systemic inflammation, opsonization of microbes, direct lysis of bacteria, clearance of immune complexes and apoptotic cells from tissues, and the generation of short-lived and long-lived memory B-cells and T-cells [36–37].

The most potent complement peptide, C5a, is a 74-residue glycopeptide that exhibits a number of ideal immunostimulatory activities including the receptor-mediated activation of monocytes and macrophages through C5a receptor 1 (C5aR1/CD88) [38] and the generation of long-lived adaptive immune responses [39–40]. C5a, however, is also a principal mediator of local and systemic inflammation through its ability to activate and recruit neutrophils, induce spasmogenesis, increase vascular permeability, and stimulate the secretion of secondary inflammatory mediators from a wide range of cell types [41]. Furthermore, many diseases caused by chronic inflammation have been linked to C5a and neutrophils [42–43] and C5a-activated neutrophils directly damage endothelial and mesothelial tissues [44–45]. As such, C5aR1 agonists that selectively activate mononuclear phagocytes over neutrophils are likely to be safer than indiscriminate C5aR1 agonists [46].

To begin developing complement peptide-derived immunostimulants (CPDI), we first identified the last 10 amino acid residues from the C-terminus activation region of human C5a ($C5a_{65\text{-}74}$: Ile^{65}-Ser^{66}-His^{67}-Lys^{68}-Asp^{69}-Met^{70}-Gln^{71}-Leu^{72}-Gly^{73}-Arg^{74}) as the minimal pharmacophore required for stimulating Guinea pig ileal contraction (surrogate for activation of mammalian macrophages) but 5-orders of magnitude less potent than native human C5a (155 μM vs. 8.7 nM) [47]. Screening for amino acid residue substitutions within $C5a_{65\text{-}74}$ that selectively increase contraction of human umbilical arteries (surrogate for activation of human macrophages) [48] over the secretion of β-glucuronidase from human

polymorphonuclear leukocytes (PMN) (surrogate for activation of human neutrophils), we identified EP54 ([Tyr^{65}Phe^{67}Pro^{69}Pro^{71}D-Ala^{73}]C5a$_{65-74}$) (Table 1) as a first-generation, C5a-derived decapeptide agonist of C5aR1 that selectively increases the potency of C5a$_{65-74}$ 775-fold in human umbilical arteries (155 μM to 200 nM) but only ~64-fold in human PMN (>300 μM to 4.7 μM) (UA/PMN selectivity = 34) [49]. Importantly, systemic immunization with EP54 directly conjugated to the C-terminal of peptide epitopes increases epitope-specific antibodies and CD8$^+$ T-cells in mice (Ab, CD8$^+$ T-cells) and rabbits (Ab), indicating that EP54 is an immunostimulant molecule that increases the generation of B-cell and T-cell adaptive immune responses [39, 50].

Pro amino acid residue substitutions at positions 5 and 7 (Positions 69 and 71 in C5a$_{65-74}$) (Table 1) likely contribute to the immunostimulatory potency and mononuclear phagocyte selectivity of EP54 by extending the peptide backbone but eliminate potential side-chain contributions by the substituted Asp^5 and Gln^7 residues [49, 51–52]. Given that adding methyl groups to backbone amide nitrogen atoms extends the peptide backbone without removing contributions of adjacent side-chains, we next screened N-methylated backbone analogs of EP54 and identified a second-generation C5a-derived decapeptide agonist of C5aR1, EP67 ([Tyr^{65}Phe^{67}Pro^{71}Me-Leu^{72}D-Ala^{73}]C5a$_{65-74}$) (Table 1), as a more potent and mononuclear phagocyte-selective immunostimulant molecule that increases the potency of C5a$_{65-74}$ 1107-fold in human umbilical arteries (155 μM to 140 nM) but only ~1.6-fold in human PMN (>300 μM to 190 μM) (UA/PMN selectivity = 2951) [53].

Systemic immunization with EP67 directly conjugated to whole protein [38], peptide epitopes [50], or attenuated pathogens [54–55] generates Th1- and Th17-biased adaptive immune responses in young and old mice [56]. Respiratory immunization with EP67 directly conjugated to peptide epitopes alone [57–58] or indirectly conjugated to encapsulated protein vaccines on the surface of biodegradable nanoparticles [11] also increases the generation of long-lived mucosal and systemic memory CD8$^+$ T-cells and subsequent protection against primary respiratory challenge in mice. Furthermore, combination respiratory/systemic immunization with EP67 directly conjugated to an amphipathic polymer solubilizer (APol) combined with CpG and Montanide increases the magnitude and quality of B-cell and T-cell adaptive immune responses generated by a protective APol-solubilized membrane protein and subsequent protection of naïve mice against primary respiratory challenge with *C. trachomatis* [59]. In addition to acting as a systemic and mucosal adjuvant, respiratory administration of EP67 alone within a 24-hour window before or after respiratory challenge also increases protection of naïve mice against primary mucosal infection with influenza [60].

Although EP67 is a promising candidate for the development of novel vaccines and adjunct immunotherapies, inefficient coupling efficiency between Pro^7 and Me-Leu^8 (Positions 71 and 72 in C5a$_{65-74}$) (Table 1) and challenging purification by HPLC greatly increase scale-up costs for clinical use. Pro^7 and Me-Leu^8, however, likely induce structural changes to the peptide backbone of EP67 that increase potency and selectivity over first-generation EP54 [53]. As such, we wanted to determine if we could overcome the scale-up challenges of EP67 by replacing Pro^7 and/or Me-Leu^8 with large-scale amenable amino acid residues that induce similar structural changes and, consequently, preserve the activity of EP67.

The NMR structure of C5a alone or as a part of inactive C5 is a four-helix core stabilized by three disulfide bridges [35] that consists of a receptor recognition region and a C-terminus activation region that contains the minimal pharmacophore, $C5a_{65-74}$ [35]. Crystallographic and NMR studies show that the C-terminus activation region has an alpha-helical structure when part of C5 but an extended, flexible structure when part of C5a [35, 61]. Recent Cryo-EM studies further show that the receptor recognition region retains its alpha-helical structure when part of C5, whereas the C-terminus activation region likely changes conformation following conversion to C5a because it is not held in place by the disulfide bridges [62]. These data suggest that the more potent form of $C5a_{65-74}$, in contrast to the helical structure observed in C5, is an extended, flexible structure that more effectively engages the activation site of C5aR1.

The major cluster view and RMSD trace of $C5a_{65-74}$ alone vs. an alpha-helical structure from *de novo* structure prediction showed long periods of low RMSD to the major cluster, suggesting that $C5a_{65-74}$ maintains an alpha-helical backbone conformation in solution (Figure 1). In contrast to $C5a_{65-74}$, although [Cha^7Leu^8]EP67 is masked in the major cluster view (Figure 1A), RMSD traces suggest that EP67 has a more flexible structure in solution that is maintained by replacing Pro^7 with the bulky trans-amino acid residue cyclohexylalanine (Cha) and/or replacing Me-Leu^7 with Leu (Figure 1B). Thus, we hypothesized that replacing Pro^7 and/or *N*-methyl Leu^8 with Cha and/or Leu amino acid residues, respectively, will not adversely affect the activity of EP67. To test this hypothesis, we compared EP67 potency, efficacy, and selective activation of human mononuclear phagocytes (monocytes, unpolarized (M0)-monocyte-derived macrophages, immature monocyte-derived dendritic cells) over human neutrophils with Cha^7 / Leu^8 analogs of EP67.

RESULTS AND DISCUSSION

Replacing Pro^7 with Cha and/or *N*-methyl Leu^8 with Leu selectively affects the potency and efficacy of EP67 in primary human mononuclear phagocytes

To determine if replacing Pro^7 and/or *N*-methyl Leu^8 with large-scale amenable amino acid residues predicted to induce similar structural changes affects the potency and efficacy of EP67 in human mononuclear phagocytes, we replaced Pro^7 with Cha ([Cha^7]EP67), Me-Leu^8 with native Leu ([Leu^8]EP67), or Pro^7 and Me-Leu^8 with Cha and native Leu, respectively ([Cha^7Leu^8]EP67) (Table 1), determined purity (Table S4), and confirmed the molecular mass (Table S5) and amino acid residue composition (Table S6) of each purified peptide. We then prepared human $CD14^+$ / $CD14^+CD16^+$ monocytes (MC) (>97% purity by flow cytometry, not shown), unpolarized human monocyte-derived macrophages (M0-MDM), and immature human monocyte-derived dendritic cells (MDDC) from the whole blood of healthy, human adult male donors (Figure 2) and compared dose-dependent secretion of IL-1β, IL-6, and TNF-α after treating with pooled human C5a desArg (parent molecule), EP54, EP67, or EP67 analogs for 24 h. IL-1β, IL-6, and TNF-α are characteristic surrogate markers for the activation of mononuclear phagocytes because they are secreted by activated tissue-resident macrophages, dendritic cells, and recruited inflammatory

monocytes during the early stages of infection to drive acute inflammation in support of innate and adaptive immune responses [33, 63].

Sigmoidal dose-response curves were observed for IL-1β secretion from MC, M0-MDM, and MDDC over the concentration range of human C5a desArg (Figure S1), whereas IL-1β was not detected after treatment with up to 1 mM EP54, EP67, or EP67 analogs (not shown). In contrast to IL-1β, sigmoidal dose-response curves were observed for IL-6 and TNF-α secretion from MC, M0-MDM, and MDDC over the concentration ranges of C5a desArg (Figure 3, black circles), EP54 (Figure 3, black squares), EP67 (black triangles), and EP67 analogs (Figure 3, colored open symbols). This suggests the current C5a-derived immunostimulants, in contrast to the C5a/C5a desArg parent molecule, do not stimulate the secretion of IL-1β from human mononuclear phagocytes. Given that C5aR1 is a G protein-coupled receptor (GPCR), one possibility is that EP67 and EP67 analogs act as "biased agonists" of C5aR1 in mononuclear phagocytes that stabilize unique active C5aR1 conformations which alter the extent of Gα and β-Arrestin coupling, the rate of GTP binding by Gα, G-protein turnover, activation of downstream signaling targets, and GPCR regulation compared to C5a/C5a desArg [64]. This possibility is supported by the recent discovery of a hexapeptide ($C5a^{pep}$) with high affinity for C5aR1 that exhibits biased agonism of neutrophil migration relative to C5a through decreased β-Arrestin coupling and C5aR1 receptor trafficking [65].

The EC_{50} of EP67 in MC, M0-MDM, and MDDC (Figure 4A, black triangles) ranged from 14.6- to 89.5-fold greater than C5a desArg (Figure 4A, black circles), whereas EC_{50} for EP54 (Figure 4A, black squares) ranged from 22.5- to 123.3-fold greater than C5a desArg, depending on the secreted cytokine and mononuclear phagocyte (Table S1). Furthermore, the EC_{50} of EP67 (Figure 4A, black triangles) was similar to the EC_{50} of EP54 (Figure 4A, black squares), with the exception of TNF-α secretion from MC (35% less) (121 ± [−0.2,+0.3] [95% CI] vs. 186 [−0.2,+0.3] nM) and IL-6 secretion from M0-MDM (47% less) (167 ± [−0.3,+0.3] [95% CI] vs. 317 [−0.9,+1] nM) (Table S1). Similar magnitudes of potencies for recombinant human C5a (EC_{50} 5 nM), EP67 (EC_{50} 140 nM), and EP54 (EC_{50} 220 nM) were reported for the contraction of human umbilical arteries (surrogate for activation of human macrophages) [53].

The E_{MAX} of EP67 (Figure 4B, black triangles), with the exception of a similar E_{MAX} for TNF-α from M0-MDM, ranged from 6 to 27% lower than C5a desArg (Figure 4B, black circles), whereas the E_{MAX} of EP54 (Figure 4B, black squares) ranged from 24 to 47% lower than C5a desArg depending on the secreted cytokine and mononuclear phagocyte (Table S1). Thus, EP67 and EP54 are both partial agonists for activating human mononuclear phagocytes compared to pooled human C5a desArg.

The E_{MAX} of EP67 (Figure 4B, black triangles) was 23.6% to 34% greater than the E_{MAX} of EP54 (Figure 4B, black squares) also depending on the secreted cytokine and mononuclear phagocyte. These results indicate that the potency of EP67 is similar or greater than EP54 depending on the secreted cytokine and mononuclear phagocyte, whereas the efficacy of EP67 for IL-6 and TNF-α secretion is greater than EP54 in human mononuclear phagocytes.

[Cha^7]EP67 (Figure 4A, red open circles) did not affect the EC_{50} of EP67 (Figure 4A, black triangles) for IL-6 and TNF-α from MC, decreased EC_{50} for IL-6 (29%) but not TNF-α from M0-MDM, and did not affect EC_{50} for IL-6 and TNF-α from MDDC. [Leu^8]EP67 (Figure 4A, green open squares) did not affect the EC_{50} of EP67 for IL-6 and TNF-α from MC, M0-MDM, or MDDC. [Cha^{7}Leu^8]EP67 (Figure 4A, blue open triangles) did not affect the EC_{50} of EP67 for IL-6 and TNF-α from MC, decreased EC_{50} for IL-6 (31%) without affecting EC_{50} for TNF-α from M0-MDM, and did not affect EC_{50} for IL-6 but decreased EC_{50} for TNF-α (39%) from MDDC. Thus, [Cha^7]EP67 selectively increases EP67 potency in M0-MDM without affecting potency in MC or MDDC, [Leu^8]EP67 does not affect EP67 potency in MC, M0-MDM, or MDDC, and [Cha^{7}Leu^8]EP67 selectively increases EP67 potency in M0-MDM and MDDC without affecting potency in MC (Table 2).

[Cha^7]EP67 (Figure 4B, red open circles) did not affect the E_{MAX} of EP67 (Figure 4B, black triangles) for IL-6 but increased E_{MAX} for TNF-α (9.5%) from MC and decreased E_{MAX} for IL-6 and TNF-α from M0-MDM (9.5%, 16%) and MDDC (5.2%, 16.6%). [Leu^8]EP67 (Figure 4B, green open squares) decreased the E_{MAX} of EP67 for IL-6 (9.3%) without affecting E_{MAX} for TNF-α from MC, did not affect E_{MAX} for IL-6 but decreased E_{MAX} for TNF-α (23%) from M0-MDM, and, surprisingly, greatly increased E_{MAX} for IL-6 and TNF-α from MDDC (41%, 45%) to levels similar (IL-6) or greater (TNF-α) than C5a desArg (Figure 4B, black circles). [Cha^{7}Leu^8]EP67 (Figure 4B, blue open triangles) did not affect the E_{MAX} of EP67 for IL-6 and TNF-α from MC, but decreased E_{MAX} for IL-6 and TNF-α from M0-MDM (21%, 21%) and MDDC (16%, 10%), respectively. Thus, [Cha^7]EP67 selectively increases EP67 efficacy in MC but decreases efficacy in M0-MDM and MDDC, [Leu^8]EP67 selectively decreases EP67 efficacy in MC and M0-MDM but significantly increases efficacy in MDDC, whereas [Cha^{7}Leu^8]EP67 does not affect EP67 efficacy in MC but decreases efficacy in M0-MDM and MDDC.

In summary (Table 2), (i.) [Cha^7]EP67 does not affect potency but selectively increases EP67 efficacy in MC, selectively increases potency but decreases EP67 efficacy in M0-MDM, and does not affect potency but decreases EP67 efficacy in MDDC (ii.) [Leu^8]EP67 does not affect potency in MC, M0-MDM, or MDDC but selectively decreases EP67 efficacy in MC and M0-MDM and greatly increases efficacy in MDDC and (iii.) [Cha^{7}Leu^8]EP67 does not affect EP67 potency or efficacy in MC, selectively increases potency but decreases EP67 efficacy in M0-MDM, and selectively increases potency but decreases EP67 efficacy in MDDC. Thus, replacing Pro^7 with Cha and/or N-methyl Leu^8 with Leu affects the potency and efficacy of EP67 depending on the secreted cytokine and human mononuclear phagocyte. These observations, like the inability to stimulate the secretion of IL-1β at up to 1 mM, are consistent with the possibility that EP67 and EP67 analogs act as biased agonists of C5aR1 in mononuclear phagocytes compared to C5a desArg.

Replacing Pro^7 with Cha and/or Me-Leu^8 with Leu does not affect potency but selectively decreases the efficacy of EP67 in primary human neutrophils

To determine if replacing Pro^7 with Cha and/or Me-Leu^8 with Leu affects the potency and efficacy of EP67 in human neutrophils (NP), we isolated human neutrophils (NP) from the

whole blood of healthy, human adult male donors (>94% purity by flow cytometry, not shown) (Figure 2) then compared dose-dependent secretion of myeloperoxidase (MPO) from NP after treating with pooled human C5a desArg, EP54, EP67, or EP67 analogs for 24 h (Figure 5). Sigmoidal dose-response curves were observed for MPO secretion from NP over the concentration ranges of C5a desArg, EP54, EP67, and EP67 analogs (Figure 5A).

The EC_{50} of EP67 for MPO secretion from NP (Figure 5B, black triangle) was 22,857-fold greater than C5a desArg (Figure 5C, black circle) (160 [−17,+20] μM vs. 7 ± 1 nM [95% CI]), whereas the EC_{50} of EP54 (Figure 5B, black square) was 3000-fold greater (21 [−3,+4] μM vs. 7 ± 1 nM [95% CI]) (Table S2). The E_{MAX} of EP67 for MPO secretion from NP (Figure 5C, black triangle) was also 62.4% less than C5a desArg (Figure 5C, black circle) (3.5 ± 0.1 [95% CI] vs. 9.3 ± 0.3 ng/mL), whereas the E_{MAX} of EP54 (Figure 5C, black square) was 39.8% less (5.6 ± 0.2 [95% CI] vs. 9.3 ± 0.3 ng/mL) (Table S2). Furthermore, the EC_{50} for EP67 was 7.6-fold greater than EP54 (160 [−17,+20] [95% CI] vs. 21 [−3,+4] μM) and the E_{MAX} was 60% less than EP54 (3.5 ± 0.1 [95% CI] vs. 5.6 ± 0.2 ng/mL) in NP (Table S2). Similar potencies for MPO secretion from human PMNs (surrogate for activation of human neutrophils) were reported for recombinant human C5a (EC_{50} 6 μM), EP54 (EC_{50} 4.4 μM), and EP67 (EC_{50} 190 μM) [53]. Thus, consistent with previous studies, (i.) the potency of EP67 and EP54 is well below the potency of human C5a desArg in human neutrophils and (ii.) EP67 is less potent and efficacious in human neutrophils than EP54.

None of the EP67 analogs (Figure 5B, colored open symbols) affected the EC_{50} of EP67 for MPO secretion from NP (Figure 5B, black triangle). In contrast, [Cha^7]EP67 (Figure 5C, red open circle) and [Cha^7Leu^8]EP67 (Figure 5C, blue open triangle) decreased the E_{MAX} of EP67 (Figure 5C, black triangle) for MPO secretion by 20% (2.8 ± 0.1 [95% CI] vs. 3.5 ± 0.2 ng/mL) and 26% (2.6 ± 0.1 [95% CI] vs. 3.5 ± 0.2 ng/mL), respectively (Table S2), whereas [Leu^8]EP67 (Figure 5C, green open square) had a similar E_{MAX} compared to EP67. Thus, replacing Pro^7 with Cha and/or N-methyl Leu^8 with Leu does not affect EP67 potency but selectively decreases efficacy in human neutrophils (Table 2). These observations, like differences in potency and efficacy observed in mononuclear phagocytes, are consistent with the possibility that EP67 and EP67 analogs act as biased agonists of C5aR1 in both mononuclear phagocytes and neutrophils compared to C5a desArg.

Replacing Pro^7 with Cha and/or Me-Leu^8 with Leu does not affect selective activation of primary human mononuclear phagocytes over human neutrophils by EP67

To determine if replacing Pro^7 with Cha and/or Me-Leu^8 with Leu affects the selective activation of human mononuclear phagocytes over human neutrophils, we compared the selective stimulation of IL-6 or TNF-α secretion from human MC, M0-MDM, and MDDC over secretion of MPO from human NP 24 h after treatment with EP54, EP67, or EP67 analogs vs. pooled human C5a desArg (Figure 6). The selectivity of EP67 for stimulating MC, M0-MDM, and MDDC over NP vs. C5a desArg (Figure 6, black triangles) ranged from 302 to 1413, whereas the selectivity of EP54 vs. C5a desArg (Figure 6, black squares) ranged from 23 to 126, depending on the secreted cytokine and mononuclear phagocyte (Table S3). Furthermore, selectivities of EP67 (Figure 6, black triangles) were 9- to 15-fold greater than EP54 (Figure 6, black squares) within the same cell type, again depending on

the secreted cytokine and mononuclear phagocyte (Table S3). Thus, EP67 selectivity for stimulating human mononuclear phagocytes over human neutrophils vs. pooled human C5a desArg is lower than the selective activation of human umbilical artery contraction (surrogate for activation of human macrophages) over human PMNs (surrogate for activation of human neutrophils) but still much greater than EP54. A much higher selectivity for stimulating the contraction of human umbilical arteries activation over MPO secretion from human PMNs was reported for EP67 (2951), whereas a similar low selectivity was reported for EP54 (34) [53]. This may be due to differences between EP67 activity in whole tissues vs. isolated cells.

None of the EP67 analogs (Figure 6, colored open symbols) affected the selectivities of EP67 for stimulating IL-6 or TNF-α secretion from MC (Figure 6A), M0-MDM (Figure 6B), or MDDC (Figure 6C) over stimulating the secretion of MPO from NP (Figure 6C, black triangles) (Table S3). Thus, replacing Pro^7 with Cha and/or N-methyl Leu^8 with Leu does not affect the selective activation of human mononuclear phagocytes over human neutrophils by EP67 vs. pooled human C5a desArg.

CONCLUSION

We found that that replacing Pro^7 with Cha and/or $Me\text{-}Leu^8$ with Leu (i.) selectively affects EP67 potency and efficacy depending on the human mononuclear phagocyte and secreted cytokine, (ii.) does not affect EP67 potency but selectively decreases efficacy in human neutrophils, and (iii.) does not affect selective activation of human mononuclear phagocytes over human neutrophils. Thus, replacing Pro^7 and $Me\text{-}Leu^8$ with large-scale amenable amino acid residues predicted to induce similar structural changes is a suitable strategy to overcome scale-up challenges with EP67.

METHODS

Experimental Methods

Peptide synthesis, purification, and characterizations—Using an AAPPTEC Apex 396 Synthesizer, all peptides were assembled on preloaded Fmoc-Arg(pbf)-Wang resin using Fmoc-amino acid derivatives and N-(dimethylamino)-1H-1,2,3-triazolo-[4,5-b]pyridin-1-ylmethylene]-N-methylmethanaminium hexafluorophosphate N-oxide (HATU) in the presence of excess DIEA. A solution of piperidine in DMF (1/4, v/v) was used to remove the Fmoc-group. Peptides were cleaved from the resin and freed of sidechain protecting groups by stirring the peptide-resin in a mixture of TFA (87.5%), phenol (5%), water (5%), and triisopropylsilane (2.5%) for 2h at room temperature. Crude products were purified by preparative reversed-phase high performance liquid chromatography (RP-HPLC) on C18-bonded silica columns under optimized gradient elution conditions employing 0.25N triethylammonium phosphate, pH 2.25 (buffer A) and a mixture of buffer A and acetonitrile (3/2, v/v, buffer B) [66]. Peptides were loaded onto the same column, previously equilibrated with a mixture of 10 mM hydrochloric acid and acetonitrile (95/5, v/v), and quickly eluted by raising the amount of acetonitrile in the eluent to 60% over 30 minutes to produce the hydrochloride salt.

Peptide purity was determined by analytical reversed-phase HPLC using three different columns with the same gradient elution conditions: an ACE 5 C18-300 column (250 x 4.6 mm, 5 μm, 300 Å pore size, catalog number ACE-221-2546), ACE 5 Phenyl-300 column (250 x 4.6 mm, 5 μm, 300 Å pore size, catalog number ACE-225-2546) and ACE 5 CN-300 column (250 x 4.6 mm, 5 μm, 300 Å pore size, catalog number. ACE-224-2546) from MAC-MOD Analytical Inc. (Chadds Ford, PA). Solvent A was water containing 0.1% trifluoroacetic acid (TFA, v/v) and solvent B was a mixture of acetonitrile and water (3/2, v/v) containing 0.1 % TFA. Peptides were eluted from the columns by increasing the percentage of solvent B from 5 to 100% over 50 minutes and column effluent was continuously monitored at 214 nm. Peptide masses were measured on an Orbitrap Fusion Lumos from ThermoScientific (Waltham MA) and with ≤ 0.5 ppm error (Mass Spectrometry and Proteomics Core Facility at the University of Nebraska Medical Center). Amino acid compositions of all peptides were determined using a Hitachi 8800 Amino Acid Analyzer after being subjected to vapor-phase hydrolysis in constant boiling 6M hydrochloric acid for 24 hours (Protein Structure Core Facility at the University of Nebraska Medical Center).

Peptide structure prediction—PEP-FOLD [67] was used to generate the initial conformation of $C5a_{65\text{-}74}$. Analogs of $C5a_{65\text{-}74}$ were generated in YASARA (www.yasara.org) and refined for 500 ps using the built-in md_refine macro. Each refined structure was then used in a 50 ns molecular dynamics (MD) simulation. All molecular dynamics simulations and post-analysis used Desmond [68] as bundled with the Schrodinger software suite. Each peptide was placed in a cubic box with periodic boundaries. No dimension of the box was allowed closer than 12 Angstroms to allow the peptides room to unfold. The box was filled with TIP4P water and neutralized by adding the appropriate Na+ or Cl− ions. Salt concentration in the box was set to 0.05 M NaCl. All simulations first used Schrodinger's built in relaxation protocol before the main MD run. The main 50 ns MD run was an NPT ensemble with temperature at 298K and pressure at 1 atm. Noose-Hoover chain and Martyna-Tobias-Klein were the thermostat and barostat methods, respectively. The average structure of the major cluster of each trajectory was then extracted for comparison in YASARA.

Isolation of human monocytes and neutrophils from human whole blood—Fresh whole blood [1 unit = 450 mL] was drawn from healthy human male donors (aged 19–40 years) into vacutainer bags containing EDTA (Innovative Research, USA). $CD14^+$, $CD14^+/CD16^+$ monocytes were isolated from whole blood [180 mL/donor] using magnetic StraightFrom® Whole Blood CD14 MicroBeads (Miltenyi Biotec, Germany) according to the manufacturer's protocol and counted (Auto T4, Nexcelom). Isolated monocytes were plated in 24-well plates [$1x10^6$ cells/well] (BD Biosciences) with complete culture medium (CCM) [1 mL] [RPMI 1640, 2 mM L-glutamine, 1% autologous plasma, 1 mM sodium pyruvate, 0.1 mM non-essential amino acids, 1x vitamins, 100 U/mL penicillin G, 100 μg/mL streptomycin sulfate; Invitrogen, USA] and incubated [37°C / 5%CO_2]. After 2 h, media was aspirated and adherent cells were washed 2X with sterile D-PBS [1 mL] ["PBS" without Ca^{2+} or Mg^{2+}, GE Healthcare Life Sciences: SH30028.02] before (i.) adding CCM alone [1 mL] or CCM containing increasing concentrations of the indicated immunostimulant and incubating for 24 h, or (ii.) adding CCM [1 mL] containing the

required concentrations of factors for differentiation into macrophages or dendritic cells over 6 days (described below).

Neutrophils were isolated from the same donors [10 mL of blood/donor] using the MACSxpress® Whole Blood Neutrophil Isolation Kit, a MACSmix™ Tube Rotator, and a MACSxpress Separator (Miltenyi Biotec, Germany) according to the manufacturer's protocol and counted (Auto T4, Nexcelom). Isolated neutrophils were plated in 24-well plates [$1x10^6$ cells/well] with CCM [1 mL] and incubated [37°C / 5%CO_2]. After 2 h, media was aspirated and adherent cells were washed 2X with sterile D-PBS [1 mL] before adding CCM alone [1 mL] or CCM containing increasing concentrations of the indicated immunostimulant.

The purity of isolated monocytes and neutrophils was determined on the day of isolation by staining cells with recombinant CD14-PE-Vio615, CD-15APC, and CD-16PE human antibodies (Miltenyi Biotec, Germany) before and after separation and analyzing by flow cytometry. Isolated cells [$1x10^6$] were resuspended in cell staining buffer (BD Biosciences) [0.100 mL] and containing the indicated antibodies [5 μL/each antibody]. Cells were gently mixed, incubated in the dark [2–8 °C, 10 min.], pelleted [300 RC, RT, 10 min], resuspended in staining buffer [1 mL], pelleted [300 RCF, RT, 10 min.], and resuspended in FACS staining buffer [0.5 mL] for analysis by flow cytometry. Cells were analyzed on a BD LSR II flow cytometer (Becton and Dickinson, La Jolla, CA) with BD High Throughput Sampler. Flow cytometer was compensated using single stained cells, maximum number of events were acquired and analyzed by FlowJo software (Tree Star, Ashland, OR, USA).

Generation of unpolarized human monocyte-derived macrophages (M0-MDM) and immature human monocyte-derived dendritic cells (MDDC)—Unpolarized human monocyte-derived macrophages (M0-MDM) were generated by culturing freshly isolated monocytes in 24-well plates [$1×10^6$ cells/well] with CCM [1 mL] containing recombinant human M-CSF (rhM-CSF, Miltenyi Biotec) [50 ng/mL] for three days, replacing half the media [0.5 mL] from each well with fresh CCM [0.5 mL] and rhM-CSF [50 ng/mL], and incubating for another 3 days [69]. Immature human monocytes-derived dendritic cells (MDDC) were generated in the same manner as M0-MDM but incubated with CCM containing recombinant human IL-4 (rhIL-4, Miltenyi Biotec) [50 ng/mL] and recombinant human GM-CSF (Miltenyi Biotec) [160 ng/mL] [70]. On Day 7, media was aspirated, cells were washed once with warm, sterile PBS [37°C], and incubated [37°C / 5%CO_2] with CCM [1 mL] containing the indicated immunostimulant for 24 h.

Potency of EP67 analogs in human mononuclear phagocytes and neutrophils —Mononuclear phagocytes (MC, M0-MDM, MDDC) or NP were plated in 24-well plates [$1x10^6$ cells/well] as described above and incubated [37°C / 5%CO_2] with CCM [1 mL] containing serial concentrations of C5a desArg, EP54, EP67, or EP67 analogs. After 24 h, average concentrations of IL-1β, IL-6, and TNF-α [± SD] (n=2 wells from 3 independent donors) in the media of mononuclear phagocytes or average concentrations of myeloperoxidase (MPO) [± SD] (n=2 wells from 3 independent donors) in the media of NP were determined by ELISA (BioLegend, USA). The average maximal concentration of secreted protein (E_{MAX} / "efficacy") and molar concentration of peptide that stimulated 50%

E_{MAX} (EC_{50} / “potency”) [± 95%CI] was then calculated by fitting the dose-response data with a four-parameter dose-response curve where Y=Min + ($x^{Hillslope}$)*(Max-Min)/ ($x^{HillSlope}$ + $EC_{50}^{HillSlope}$) (Graphpad Prism 8).

Selective activation of human mononuclear phagocytes over neutrophils— Average selective activation of the indicated mononuclear phagocyte vs. activation of NP [± propagated 95% CI] (n=3 independent donors) by EP54, EP67, and EP67 analogs relative to C5a desArg (“selectivity”) was calculated as [antilog ((−ΔC5a desArg mononuclear phagocyte) - (−ΔC5a desArg NP))] where ΔC5a desArg = pD_2 (C5a desArg) - pD_2 (peptide) and pD_2 = −log (EC_{50}[M]) for IL-6 and TNF-a secretion from the indicated mononuclear phagocyte or MPO secretion from NP [53]. The selectivity of human C5a desArg was set to a value of 1 using this equation because it is equipotent in mononuclear phagocytes and NP. Thus, the greater the selectivity value, the greater the selective activation of mononuclear phagocytes over neutrophils relative to C5a desArg.

Supplementary Material

Refer to Web version on PubMed Central for supplementary material.

ACKNOWLEDGEMENTS

We dedicate this manuscript to the memory of Dr. Sam Sanderson, the inventor of EP54 and EP67. His larger-than-life personality, enthusiasm for research, and unwavering friendship will be greatly missed. This work was supported by NIH/NIAID 5R01AI125137 (SDS, JAV, JLV), NIH/NIAID 1R01AI121050 (JAV), the Weitz Family Foundation (SDS, JAV), NIH/OD UG1OD024953 (RJM), NIH/NIAID 5R21AI134618 (PAB), NIH/NIAID 5P01AI131568 (PAB), NIH/NIAID 1P01AI129859-01A1 (PAB), NIH/OD K01 OD023034 (SSI), NIH/NIAID R03AI138792 (SSI), NIH/NIAID 1R21AI34368 (SSI), NIH/NIAID R01AI105084 (DRR), UNMC Department of Pharmaceutical Sciences Startup (DRR), a Ministry of Education Scholarship, King Saud University (Riyadh, Saudi Arabia) (AMA), and the Holland Computing Center of the University of Nebraska (NP), which receives support from the Nebraska Research Initiative. We greatly appreciate expert technical guidance by Dr. Juliana Lewis (Miltenyi Biotec), Victoria Smith M.S. and Dr. Philip Hexley (UNMC Flow Cytometry Facility), and Dr. Laurey Steinke (UNMC Protein Structure Core Facility). The UNMC Flow Cytometry Research Facility and Protein Structure Core Facility is managed through the Office of the Vice Chancellor for Research and supported by state funds from the Nebraska Research Initiative (NRI) and The Fred and Pamela Buffet Cancer Center’s National Cancer Institute Cancer Support Grant.

ABBREVIATIONS

APC:
antigen-presenting cells

C5a:
complement component 5a

C5aR1/CD88:
C5a Receptor 1

Cha^7:
cyclohexylalanine7 amino acid residue in EP67

CPDI:
complement peptide-derived immunostimulant(s)

EP54:
1st generation decapeptide agonist of C5aR1

EP67:
2nd generation decapeptide agonist of C5aR1

GPCR:
G protein-coupled receptor

Me-Leu^8:
N-methyl-Leu^8 amino acid residue in EP67

M0-MDM:
unpolarized immature (M0)-monocyte-derived macrophages

MAC:
membrane attack complex

MC:
monocytes

MDDC:
immature monocyte-derived dendritic cells

Mononuclear phagocytes:
monocytes, macrophages, and dendritic cells

MPL:
Monophosphoryl Lipid A

PAMPs:
pattern associated molecular patterns

PMNs:
polymorphonuclear cells

PRRs:
pattern recognition receptors

RMSD:
root-mean-square deviation of atomic positions

TLR:
toll-like receptor family

REFERENCES

1. Hamborsky J; Kroger A; Wolfe C, Epidemiology and Prevention of Vaccine-Preventable Diseases. 13 ed.; Centers for Disease Control and Prevention: Washington, D.C., 2015.

2. Plotkin SA, Vaccines We Need But Don't Have. Viral Immunol 2018, 31 (2), 114–116. DOI: 10.1089/vim.2017.0126. [PubMed: 29131713]

3. Gallagher T; Lipsitch M, Post-Exposure Effects of Vaccines on Infectious Diseases. Epidemiol Rev 2019 DOI: 10.1093/epirev/mxz014.

4. Rosenthal KS; Kuntz A; Sikon J, Why Don't We Have a Vaccine Against…….? Part 2. Bacteria. Infectious Diseases in Clinical Practice 2016, 24 (2), 119–123. DOI: 10.1097/ipc.0000000000000352.

5. Rosenthal KS; Sikon J; Kuntz A, Why Don't We Have a Vaccine Against…….? Part 1. Viruses. Infectious Diseases in Clinical Practice 2015, 23 (4), 202–210. DOI: 10.1097/ipc.0000000000000264.

6. Amanna IJ; Slifka MK, Successful Vaccines In Current topics in microbiology and immunology, 2018/07/27 ed.; Springer Nature Switzerland AG: Basel, Switzerland, 2018; pp 1–30. DOI: 10.1007/82_2018_102.

7. RTS,S/AS01E malaria vaccine (MoSQUIRIX*) Children living in malaria-endemic regions: little efficacy, poorly documented harms. Prescrire Int 2017, 26 (178), 5–8. [PubMed: 30730633]

8. Nami S; Mohammadi R; Vakili M; Khezripour K; Mirzaei H; Morovati H, Fungal vaccines, mechanism of actions and immunology: A comprehensive review. Biomed Pharmacother 2019, 109, 333–344. DOI: 10.1016/j.biopha.2018.10.075. [PubMed: 30399567]

9. Nguipdop Djomo P; Thomas SL; Fine PEM, Correlates of vaccine-induced protection: methods and implications. WHO Document Production Services: Geneva, Switzerland, 2013; Vol. 1, p 1–49.

10. Plotkin SA, Complex correlates of protection after vaccination. Clinical infectious diseases : an official publication of the Infectious Diseases Society of America 2013, 56 (10), 1458–1465. DOI: 10.1093/cid/cit048. [PubMed: 23386629]

11. Tallapaka SB; Karuturi BVK; Yeapuri P; Curran SM; Sonawane YA; Phillips JA; David Smith D; Sanderson SD; Vetro JA, Surface conjugation of EP67 to biodegradable nanoparticles increases the generation of long-lived mucosal and systemic memory T-cells by encapsulated protein vaccine after respiratory immunization and subsequent T-cell-mediated protection against respiratory infection. Int J Pharm 2019, 565, 242–257. DOI: 10.1016/j.ijpharm.2019.05.012. [PubMed: 31077762]

12. Siegrist C-A, Vaccine Immunology In Vaccines, 6th ed.; Plotkin S; Orenstein W; Offit P, Eds. Elsevier: Amsterdam, Netherlands, 2012; pp 14–33.

13. Rappuoli R, Bridging the knowledge gaps in vaccine design. Nat Biotechnol 2007, 25 (12), 1361–1366. DOI: 10.1038/nbt1207-1361. [PubMed: 18066025]

14. Ionescu L; Urschel S, Memory B Cells and Long-lived Plasma Cells. Transplantation 2019, 103 (5), 890–898. DOI: 10.1097/TP.0000000000002594. [PubMed: 30747835]

15. Thakur A; Pedersen LE; Jungersen G, Immune markers and correlates of protection for vaccine induced immune responses. Vaccine 2012, 30 (33), 4907–4920. DOI: 10.1016/j.vaccine.2012.05.049. [PubMed: 22658928]

16. Amanna IJ; Slifka MK, Contributions of humoral and cellular immunity to vaccine-induced protection in humans. Virology 2011, 411 (2), 206–215. DOI: 10.1016/j.virol.2010.12.016. [PubMed: 21216425]

17. Plotkin SA, Updates on immunologic correlates of vaccine-induced protection. Vaccine 2020, 38 (9), 2250–2257. DOI: 10.1016/j.vaccine.2019.10.046. [PubMed: 31767462]

18. Vetter V; Denizer G; Friedland LR; Krishnan J; Shapiro M, Understanding modern-day vaccines: what you need to know. Ann Med 2018, 50 (2), 110–120. DOI: 10.1080/07853890.2017.1407035. [PubMed: 29172780]

19. Zepp F, Principles of vaccine design-Lessons from nature. Vaccine 2010, 28 Suppl 3, C14–24. DOI: 10.1016/j.vaccine.2010.07.020. [PubMed: 20713252]

20. Delany I; Rappuoli R; De Gregorio E, Vaccines for the 21st century. EMBO Mol Med 2014, 6 (6), 708–720. DOI: 10.1002/emmm.201403876. [PubMed: 24803000]

21. Lycke N, Recent progress in mucosal vaccine development: potential and limitations. Nature reviews. Immunology 2012, 12 (8), 592–605. DOI: 10.1038/nri3251.

22. Santos E; Levitz SM, Fungal vaccines and immunotherapeutics. Cold Spring Harb Perspect Med 2014, 4 (11), a019711 DOI: 10.1101/cshperspect.a019711. [PubMed: 25368016]

23. Brito LA; O'Hagan DT, Designing and building the next generation of improved vaccine adjuvants. Journal of controlled release : official journal of the Controlled Release Society 2014, 190, 563–579. DOI: 10.1016/j.jconrel.2014.06.027. [PubMed: 24998942]
24. McAllister MM, Successful vaccines for naturally occurring protozoal diseases of animals should guide human vaccine research. A review of protozoal vaccines and their designs. Parasitology 2014, 141 (5), 624–640. DOI: 10.1017/S0031182013002060. [PubMed: 24476952]
25. Rodrigues CMC; Pinto MV; Sadarangani M; Plotkin SA, Whither vaccines? J Infect 2017, 74 Suppl 1, S2–S9. DOI: 10.1016/S0163-4453(17)30184-6. [PubMed: 28646957]
26. Kaufmann SHE; Dorhoi A; Hotchkiss RS; Bartenschlager R, Host-directed therapies for bacterial and viral infections. Nat Rev Drug Discov 2018, 17 (1), 35–56. DOI: 10.1038/nrd.2017.162. [PubMed: 28935918]
27. Iwasaki A; Medzhitov R, Control of adaptive immunity by the innate immune system. Nature immunology 2015, 16 (4), 343–353. DOI: 10.1038/ni.3123. [PubMed: 25789684]
28. Iwasaki A; Foxman EF; Molony RD, Early local immune defences in the respiratory tract. Nature reviews. Immunology 2017, 17 (1), 7–20. DOI: 10.1038/nri.2016.117.
29. Vasou A; Sultanoglu N; Goodbourn S; Randall RE; Kostrikis LG, Targeting Pattern Recognition Receptors (PRR) for Vaccine Adjuvantation: From Synthetic PRR Agonists to the Potential of Defective Interfering Particles of Viruses. Viruses 2017, 9 (7). DOI: 10.3390/v9070186.
30. Kavathas PB; Krause PJ; Ruddle NH, Innate Immunity: Recognition and Effector Functions In Immunoepidemiology, Ruddle NH; Kavathas PB.; Krause PJ, Eds. Cham, Switzerland, 2019; pp 39–53.
31. Del Giudice G; Rappuoli R; Didierlaurent AM, Correlates of adjuvanticity: A review on adjuvants in licensed vaccines. Semin Immunol 2018, 39, 14–21. DOI: 10.1016/j.smim.2018.05.001. [PubMed: 29801750]
32. Levitz SM; Golenbock DT, Beyond empiricism: informing vaccine development through innate immunity research. Cell 2012, 148 (6), 1284–1292. DOI: 10.1016/j.cell.2012.02.012. [PubMed: 22424235]
33. Abbas AK; Lichtman AHH; Pillai S, Cellular and Molecular Immunology International Edition. Elsevier Health Sciences: Philadelphia, PA, 2017.
34. Murphy K; Weaver C, Janeway's immunobiology Garland Science, Taylor & Francis Group, LLC: New York, NY USA, 2017.
35. Klos A; Wende E; Wareham KJ; Monk PN, International Union of Basic and Clinical Pharmacology. [corrected]. LXXXVII. Complement peptide C5a, C4a, and C3a receptors. Pharmacological reviews 2013, 65 (1), 500–543. [PubMed: 23383423]
36. Noris M; Remuzzi G, Overview of complement activation and regulation. Semin Nephrol 2013, 33 (6), 479–492. DOI: 10.1016/j.semnephrol.2013.08.001. [PubMed: 24161035]
37. Killick J; Morisse G; Sieger D; Astier AL, Complement as a regulator of adaptive immunity. Semin Immunopathol 2018, 40 (1), 37–48. DOI: 10.1007/s00281-017-0644-y. [PubMed: 28842749]
38. Morgan EL; Morgan BN; Stein EA; Vitrs EL; Thoman ML; Sanderson SD; Phillips JA, Enhancement of in vivo and in vitro immune functions by a conformationally biased, response-selective agonist of human C5a: implications for a novel adjuvant in vaccine design. Vaccine 2009, 28 (2), 463–469. DOI: 10.1016/j.vaccine.2009.10.029. [PubMed: 19836478]
39. Tempero RM; Hollingsworth MA; Burdick MD; Finch AM; Taylor SM; Vogen SM; Morgan EL; Sanderson SD, Molecular adjuvant effects of a conformationally biased agonist of human C5a anaphylatoxin. Journal of immunology 1997, 158 (3), 1377–1382.
40. Dunkelberger JR; Song WC, Role and mechanism of action of complement in regulating T cell immunity. Mol Immunol 2010, 47 (13), 2176–2186. DOI: 10.1016/j.molimm.2010.05.008. [PubMed: 20603023]
41. Sanderson SD; Kirnarsky L; Sherman SA; Ember JA; Finch AM; Taylor SM, Decapeptide agonists of human C5a: the relationship between conformation and spasmogenic and platelet aggregatory activities. Journal of medicinal chemistry 1994, 37 (19), 3171–3180. [PubMed: 7932541]
42. Guo RF; Ward PA, Role of C5a in inflammatory responses. Annual review of immunology 2005, 23, 821–852. DOI: 10.1146/annurev.immunol.23.021704.115835.

43. Castanheira FVS; Kubes P, Neutrophils and NETs in modulating acute and chronic inflammation. Blood 2019, 133 (20), 2178–2185. DOI: 10.1182/blood-2018-11-844530. [PubMed: 30898862]
44. Chakraborty S; Karasu E; Huber-Lang M, Complement After Trauma: Suturing Innate and Adaptive Immunity. Frontiers in immunology 2018, 9, 2050 DOI: 10.3389/fimmu.2018.02050. [PubMed: 30319602]
45. Lohde E; Raude H; Luck M; Kraas E; Lierse W, Complement activated granulocytes can cause autologous tissue destruction in man. Mediators Inflamm 1992, 1 (3), 177–181. DOI: 10.1155/S0962935192000279. [PubMed: 18475458]
46. Short AJ; Paczkowski NJ; Vogen SM; Sanderson SD; Taylor SM, Response-selective C5a agonists: differential effects on neutropenia and hypotension in the rat. Br J Pharmacol 1999, 128 (3), 511–514. DOI: 10.1038/sj.bjp.0702847. [PubMed: 10516626]
47. Ember JA; Sanderson SD; Taylor SM; Kawahara M; Hugli TE, Biologic activity of synthetic analogues of C5a anaphylatoxin. Journal of immunology 1992, 148 (10), 3165–3173.
48. Marceau F; deBlois D; Laplante C; Petitclerc E; Pelletier G; Grose JH; Hugli TE, Contractile effect of the chemotactic factors f-Met-Leu-Phe and C5a on the human isolated umbilical artery. Role of cyclooxygenase products and tissue macrophages. Circ Res 1990, 67 (5), 1059–1070. DOI: 10.1161/01.res.67.5.1059. [PubMed: 1699682]
49. Finch AM; Vogen SM; Sherman SA; Kirnarsky L; Taylor SM; Sanderson SD, Biologically active conformer of the effector region of human C5a and modulatory effects of N-terminal receptor binding determinants on activity. Journal of medicinal chemistry 1997, 40 (6), 877–884. DOI: 10.1021/jm960727r. [PubMed: 9083476]
50. Kollessery G; Nordgren TM; Mittal AK; Joshi SS; Sanderson SD, Tumor-specific peptide-based vaccines containing the conformationally biased, response-selective C5a agonists EP54 and EP67 protect against aggressive large B cell lymphoma in a syngeneic murine model. Vaccine 2011, 29 (35), 5904–5910. DOI: 10.1016/j.vaccine.2011.06.070. [PubMed: 21723901]
51. Vogen SM; Finch AM; Wadi SK; Thatcher J; Monk PN; Taylor SM; Sanderson SD, The influence of Lys68 in decepeptide agonists of C5a on C5a receptor binding, activation and selectivity. J Pept Res 1999, 53 (1), 8–17. [PubMed: 10195437]
52. Vogen SM; Prakash O; Kirnarsky L; Sanderson SD; Sherman SA, Determination of structural elements related to the biological activities of a potent decapeptide agonist of human C5a anaphylatoxin. J Pept Res 1999, 54 (1), 74–84. [PubMed: 10448972]
53. Vogen SM; Paczkowski NJ; Kirnarsky L; Short A; Whitmore JB; Sherman SA; Taylor SM; Sanderson SD, Differential activities of decapeptide agonists of human C5a: the conformational effects of backbone N-methylation. Int Immunopharmacol 2001, 1 (12), 2151–2162. [PubMed: 11710544]
54. Hung CY; Hurtgen BJ; Bellecourt M; Sanderson SD; Morgan EL; Cole GT, An agonist of human complement fragment C5a enhances vaccine immunity against Coccidioides infection. Vaccine 2012, 30 (31), 4681–4690. DOI: 10.1016/j.vaccine.2012.04.084. [PubMed: 22575167]
55. Cole GT; Hung CY; Sanderson SD; Hurtgen BJ; Wuthrich M; Klein BS; Deepe GS; Ostroff GR; Levitz SM, Novel strategies to enhance vaccine immunity against coccidioidomycosis. PLoS pathogens 2013, 9 (12), e1003768 DOI: 10.1371/journal.ppat.1003768. [PubMed: 24367252]
56. Morgan EL; Thoman ML; Sanderson SD; Phillips JA, A novel adjuvant for vaccine development in the aged. Vaccine 2010, 28 (52), 8275–8279. DOI: 10.1016/j.vaccine.2010.10.008. [PubMed: 20965299]
57. Karuturi BV; Tallapaka SB; Phillips JA; Sanderson SD; Vetro JA, Preliminary evidence that the novel host-derived immunostimulant EP67 can act as a mucosal adjuvant. Clinical immunology 2015, 161 (2), 251–259. DOI: 10.1016/j.clim.2015.06.006. [PubMed: 26111481]
58. Karuturi BVK; Tallapaka SB; Yeapuri P; Curran SM; Sanderson SD; Vetro JA, Encapsulation of an EP67-Conjugated CTL Peptide Vaccine in Nanoscale Biodegradable Particles Increases the Efficacy of Respiratory Immunization and Affects the Magnitude and Memory Subsets of Vaccine-Generated Mucosal and Systemic CD8+ T Cells in a Diameter-Dependent Manner. Molecular pharmaceutics 2017, 14 (5), 1469–1481. DOI: 10.1021/acs.molpharmaceut.6b01088. [PubMed: 28319404]

59. Tifrea DF; Pal S; Le Bon C; Giusti F; Popot JL; Cocco MJ; Zoonens M; de la Maza LM, Co-delivery of amphipol-conjugated adjuvant with antigen, and adjuvant combinations, enhance immune protection elicited by a membrane protein-based vaccine against a mucosal challenge with Chlamydia. Vaccine 2018, 36 (45), 6640–6649. DOI: 10.1016/j.vaccine.2018.09.055. [PubMed: 30293763]
60. Sanderson SD; Thoman ML; Kis K; Virts EL; Herrera EB; Widmann S; Sepulveda H; Phillips JA, Innate immune induction and influenza protection elicited by a response-selective agonist of human C5a. PloS one 2012, 7 (7), e40303 DOI: 10.1371/journal.pone.0040303. [PubMed: 22792270]
61. Zhang X; Boyar W; Toth MJ; Wennogle L; Gonnella NC, Structural definition of the C5a C terminus by two-dimensional nuclear magnetic resonance spectroscopy. Proteins 1997, 28 (2), 261–267. DOI: 10.1002/(sici)1097-0134(199706)28:2<261::aid-prot13>3.0.co;2-g. [PubMed: 9188742]
62. Reichhardt MP; Johnson S; Tang T; Morgan T; Tebeka N; Popitsch N; Deme JC; Jore MM; Lea SM, An inhibitor of complement C5 provides structural insights into activation. Proceedings of the National Academy of Sciences of the United States of America 2020, 117 (1), 362–370. DOI: 10.1073/pnas.1909973116. [PubMed: 31871188]
63. Turner MD; Nedjai B; Hurst T; Pennington DJ, Cytokines and chemokines: At the crossroads of cell signalling and inflammatory disease. Biochim Biophys Acta 2014, 1843 (11), 2563–2582. DOI: 10.1016/j.bbamcr.2014.05.014. [PubMed: 24892271]
64. Wootten D; Christopoulos A; Marti-Solano M; Babu MM; Sexton PM, Mechanisms of signalling and biased agonism in G protein-coupled receptors. Nat Rev Mol Cell Biol 2018, 19 (10), 638–653. DOI: 10.1038/s41580-018-0049-3. [PubMed: 30104700]
65. Pandey S; Li XX; Srivastava A; Baidya M; Kumari P; Dwivedi H; Chaturvedi M; Ghosh E; Woodruff TM; Shukla AK, Partial ligand-receptor engagement yields functional bias at the human complement receptor, C5aR1. J Biol Chem 2019, 294 (24), 9416–9429. DOI: 10.1074/jbc.RA119.007485. [PubMed: 31036565]
66. Smith DD; Hanly AM, Purification of synthetic peptides by high performance liquid chromatography. Methods Mol Biol 1997, 73, 75–87. DOI: 10.1385/0-89603-399-6:75. [PubMed: 9031199]
67. Shen Y; Maupetit J; Derreumaux P; Tuffery P, Improved PEP-FOLD Approach for Peptide and Miniprotein Structure Prediction. J Chem Theory Comput 2014, 10 (10), 4745–4758. DOI: 10.1021/ct500592m. [PubMed: 26588162]
68. Bowers KJ; Chow DE; Xu H; Dror RO; Eastwood MP; Gregersen BA; Klepeis JL; Kolossvary I; Moraes MA; Sacerdoti FD; Salmon JK; Shan Y; Shaw DE In Scalable Algorithms for Molecular Dynamics Simulations on Commodity Clusters, SC '06: Proceedings of the 2006 ACM/IEEE Conference on Supercomputing, 11-17 Nov. 2006; 2006; pp 43–43. DOI: 10.1109/SC.2006.54.
69. Rey-Giraud F; Hafner M; Ries CH, In vitro generation of monocyte-derived macrophages under serum-free conditions improves their tumor promoting functions. PloS one 2012, 7 (8), e42656 DOI: 10.1371/journal.pone.0042656. [PubMed: 22880072]
70. Colic M; Jandric D; Stojic-Vukanic Z; Antic-Stankovic J; Popovic P; Vasilijic S; Milosavljevic P; Balint B, Differentiation of human dendritic cells from monocytes in vitro using granulocyte-macrophage colony stimulating factor and low concentration of interleukin-4. Vojnosanit Pregl 2003, 60 (5), 531–538. DOI: 10.2298/vsp0305531c. [PubMed: 14608830]

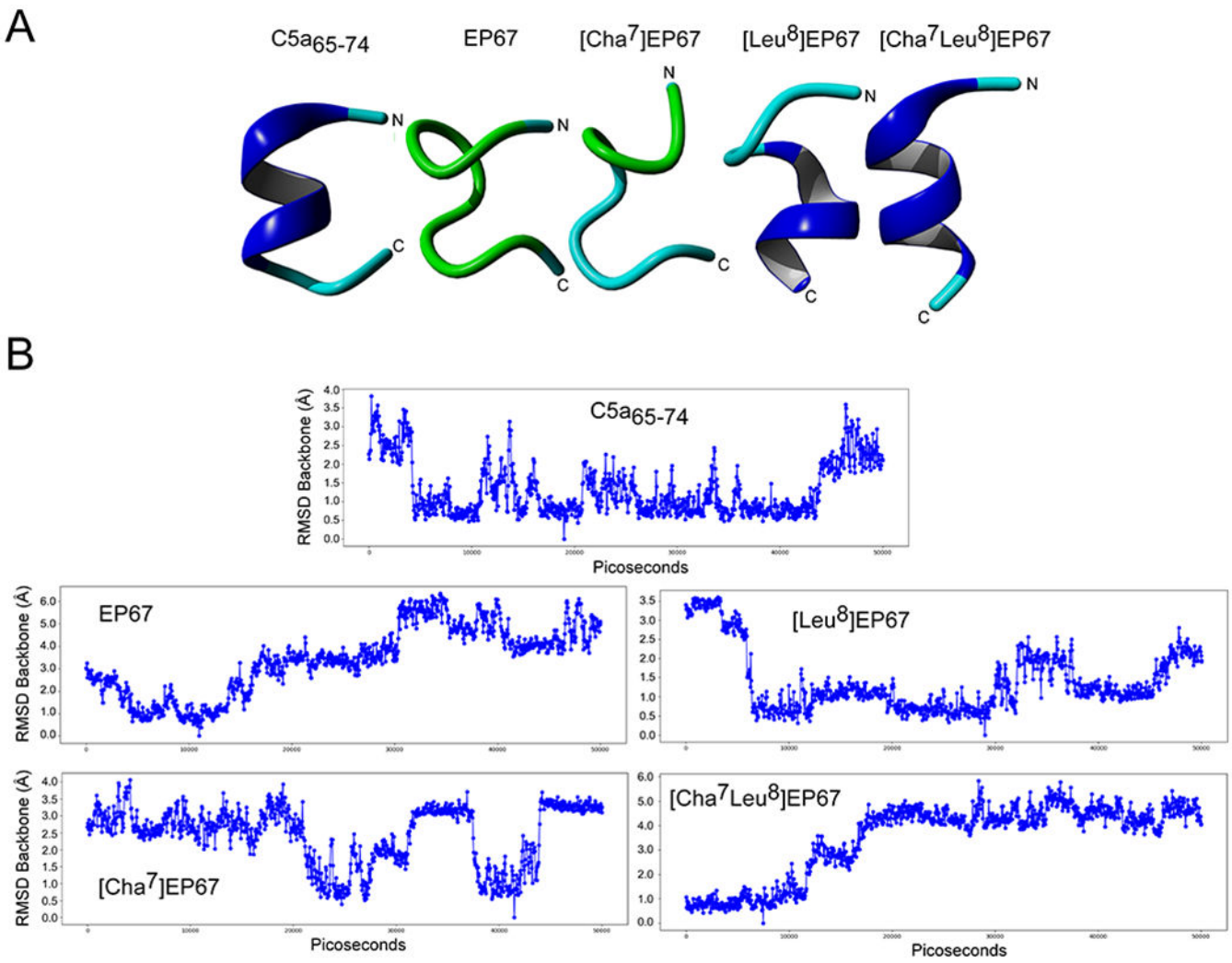

FIGURE 1. ***De novo*** **peptide structure prediction and comparison of C5a$_{65-74}$, EP67, and EP67 analog conformations.**

(A) Major cluster view and (B) RMSD traces of C5a$_{65-74}$, EP67, and EP67 analogs from an alpha-helical structure were generated by PEP-FOLD. Analogs were generated in YASARA and refined for 500 ps using the built-in md_refine macro. Each refined structure was then used in a 50 ns molecular dynamics (MD) simulation. All molecular dynamics simulations and post-analysis used Desmond as bundled with the Schrodinger software suite. Peptides were placed in a cubic box with periodic boundaries. No dimension of the box was allowed closer than 12 Angstroms to allow the peptides room to unfold. The box was filled with TIP4P water and neutralized by adding appropriate Na+ or Cl− ions. Salt concentration in the box was set to 0.05 M NaCl. All simulations first used Schrodinger's built in relaxation protocol before the main MD run. The main 50 ns MD run was an NPT ensemble with temperature at 298K and pressure at 1 atm. Noose-Hoover chain and Martyna-Tobias-Klein were the thermostat and barostat methods, respectively. The average structure of the major cluster of each trajectory was then extracted for comparison in YASARA.

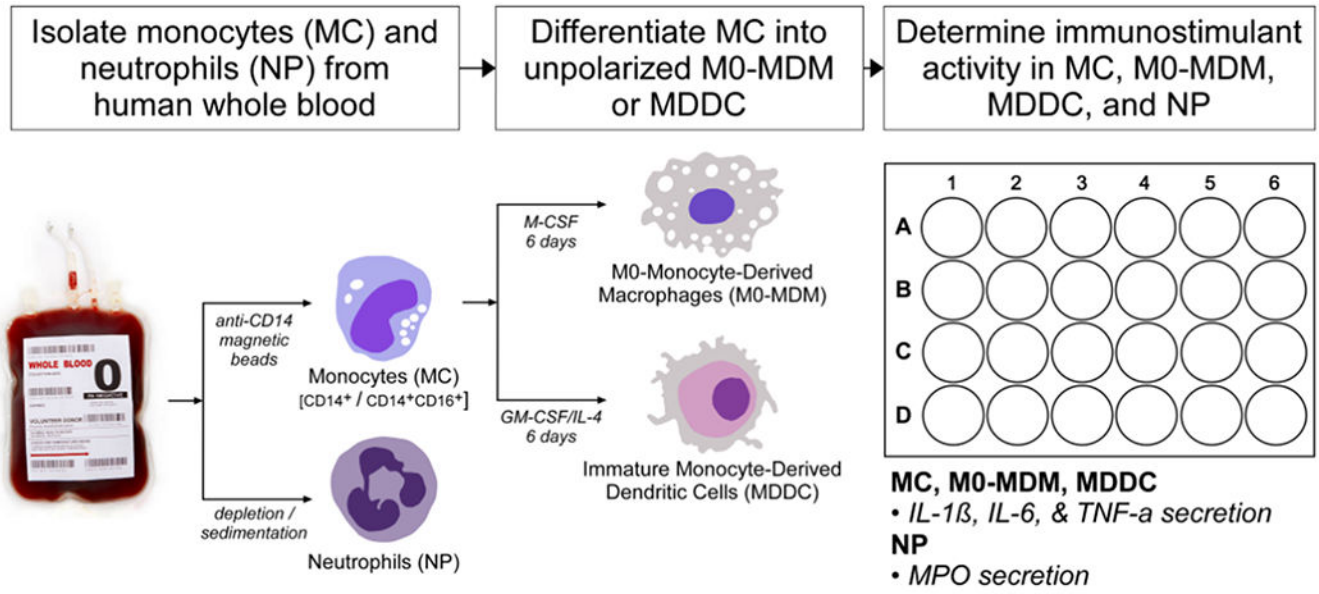

FIGURE 2. Experimental design for determining immunostimulant activity in primary human mononuclear phagocytes and neutrophils.

Monocytes (MC) and neutrophils (NP) were isolated from the whole blood of healthy, human adult male donors using Miltenyi magnetic anti-CD14 MicroBeads and MACSxpress® Whole Blood Neutrophil Isolation Kits, respectively. Isolated NP were plated for 2 h before treatment, whereas isolated $CD14^+$/$CD14^+CD16^+$ MC were plated for 2 h before immunostimulant treatment or differentiated into M0-monocyte-derived macrophages (M0-MDM) (human GM-CSF 6 d) or immature monocyte-derived dendritic cells (MDDC) (human GM-CSF/IL-4 for 7 d) before treatment. For potency studies, cells were incubated with increasing concentrations of the indicated immunostimulant for 24 h and concentrations of IL-6 and TNF-α [MC, M0-MDM, MDDC] (Figure 3) or myeloperoxidase (MPO) [NP] (Figure 5) released into cell culture media was determined by ELISA. For kinetic studies, MC, M0-MDM, and MDDC were incubated with the EC_{50} of the indicated immunostimulant in the respective cell type and concentrations IL-6 and TNF-α released into cell culture media were determined after 6, 12, 24, and 48 h by ELISA.

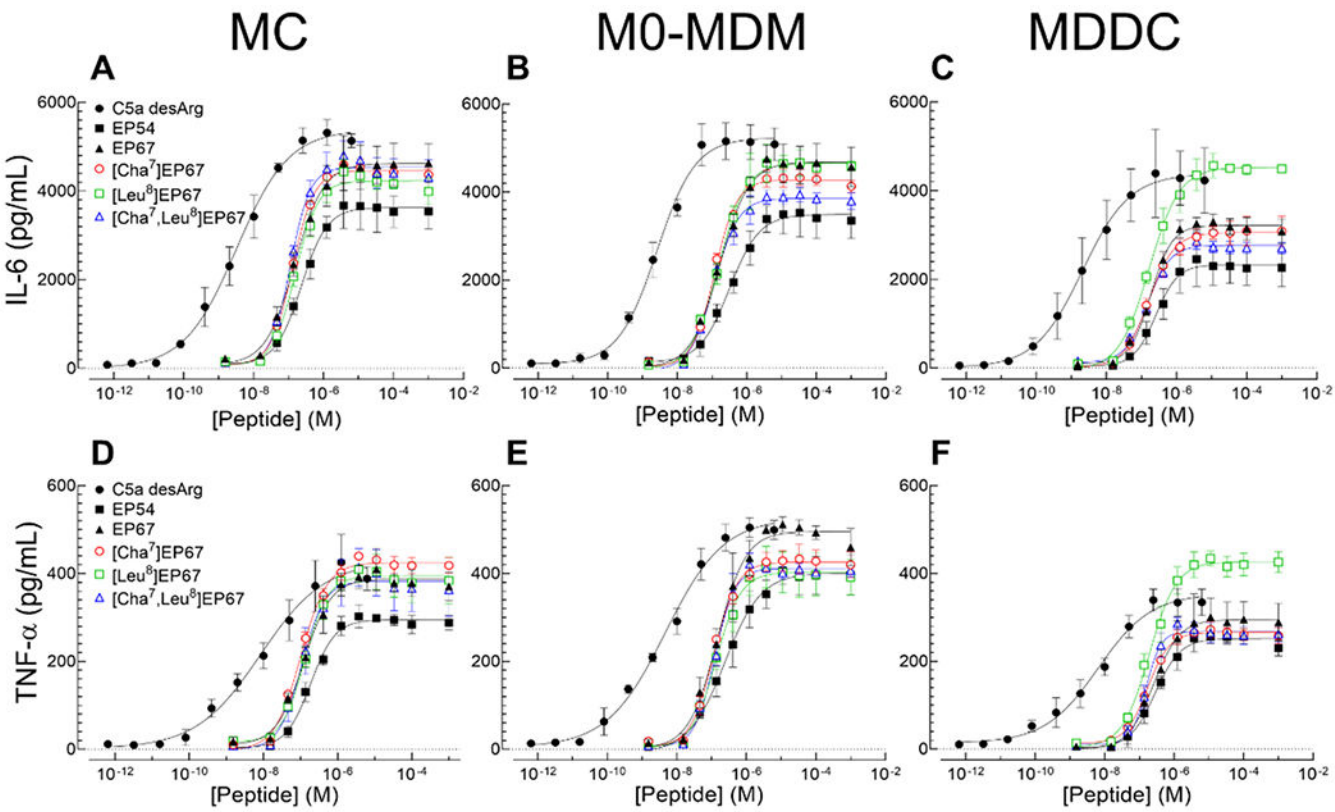

Figure 3. Dose response of IL-6 and TNF-α secretion from primary human monocytes, M0-monocyte-derived macrophages, and immature monocyte-derived dendritic cells after treatment with human C5a desArg, EP54, EP67, or EP67 analogs for 24 h.

Human monocytes (MC), unpolarized M0-monocyte-derived macrophages (M0-MDM), and immature monocyte-derived dendritic cells (MDDC) were prepared from the whole blood of healthy, human adult male donors (Figure 2). Cells (1 x 10^6) were then treated with increasing concentrations of human C5a desArg pooled from the blood of multiple donors (black circles), 1st-generation EP54 (black squares), 2^{nd}-generation EP67 (black triangles), [Cha^7]EP67 (red open circles), [Leu^8]EP67 (green open squares), or [Cha^7, Leu^8]EP67 (blue open triangles). After 24 h, average concentrations (± SD) (n=2 replicates from 3 blood donors) of IL-6 or TNF-α secreted into the cell culture media of human monocytes (**A** & **D**), M0-MDM (**B** & **E**), or MDDC (**C** & **F**) were determined by ELISA and fit with a four-parameter dose-response curve where $Y=Min + (x^{Hillslope})*(Max-Min)/(x^{HillSlope} + EC_{50}{}^{HillSlope})$.

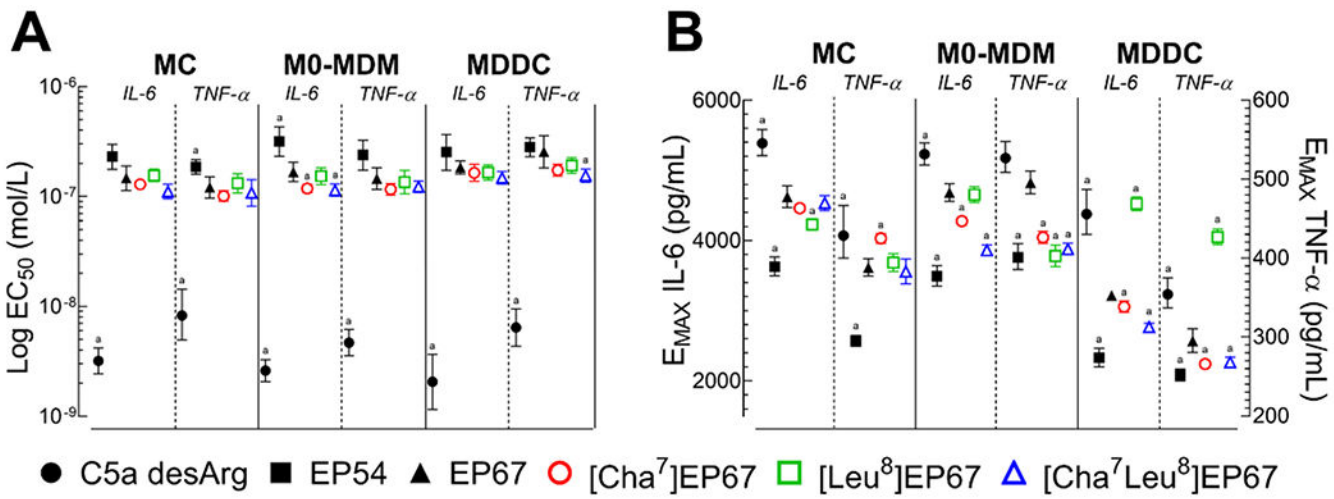

Figure 4. Comparison of potencies and efficacies for IL-6 and TNF-α secretion from primary human mononuclear phagocytes after treatment with human C5a desArg, EP54, EP67, or EP67 analogs for 24 h.

Average (**A**) EC_{50} (potencies) and (**B**) E_{MAX} (efficacies) ±95% CI for IL-6 and TNF-α were calculated (Table S1) from dose response curves of IL-6 and TNF-α secretion from human monocytes (MC), M0-monocyte-derived macrophages (M0-MDM), and monocyte-derived dendritic cells (MDDC) after treatment for 24 h (Figure 3). 0.05 level of statistical difference vs. [a]EP67 (black triangles) for the indicated cytokine and cell type.

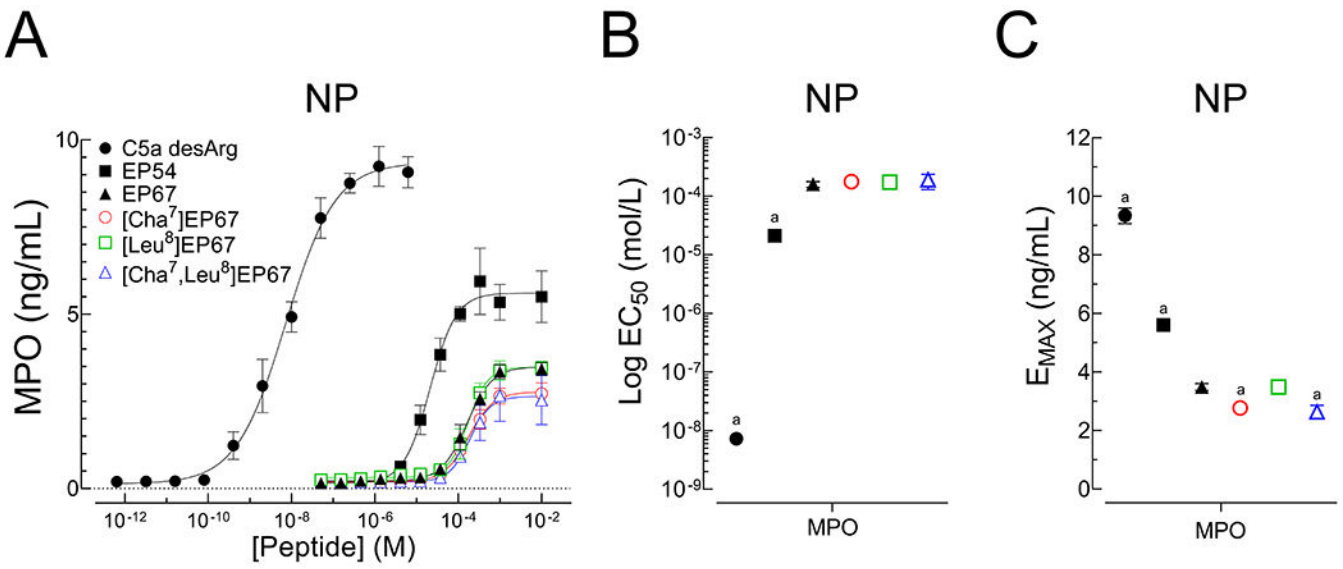

Figure 5. Comparison of potencies and efficacies for myeloperoxidase secretion from primary human neutrophils after treatment with human C5a desArg, EP54, EP67, or EP67 analogs for 24 h.

(**A**) Human neutrophils (NP) were prepared from the whole blood of healthy, human adult male donors (Figure 2). NP were then treated with increasing concentrations of human C5a desArg pooled from the blood of multiple donors (black circles), EP54 (black squares), EP67 (black triangles), [Cha^7]EP67 (open red circles), [Leu^8]EP67 (open green squares), or [Cha^7, Leu^8]EP67 (open blue triangles). After 24 h, average concentrations (± SD) (n=2 replicates from 3 blood donors) of myeloperoxidase (MPO) secreted into cell culture media were determined by ELISA and fit with a four-parameter dose-response curve where Y=Min + ($x^{Hillslope}$)*(Max-Min)/($x^{HillSlope}$ + $EC_{50}^{HillSlope}$). Average (**B**) potencies (Log EC_{50}) and (**C**) efficacies (E_{MAX}) ±95% CI for MPO secretion (Table S2) were calculated from MPO dose response curves. [a]0.05 level of statistical difference vs. EP67.

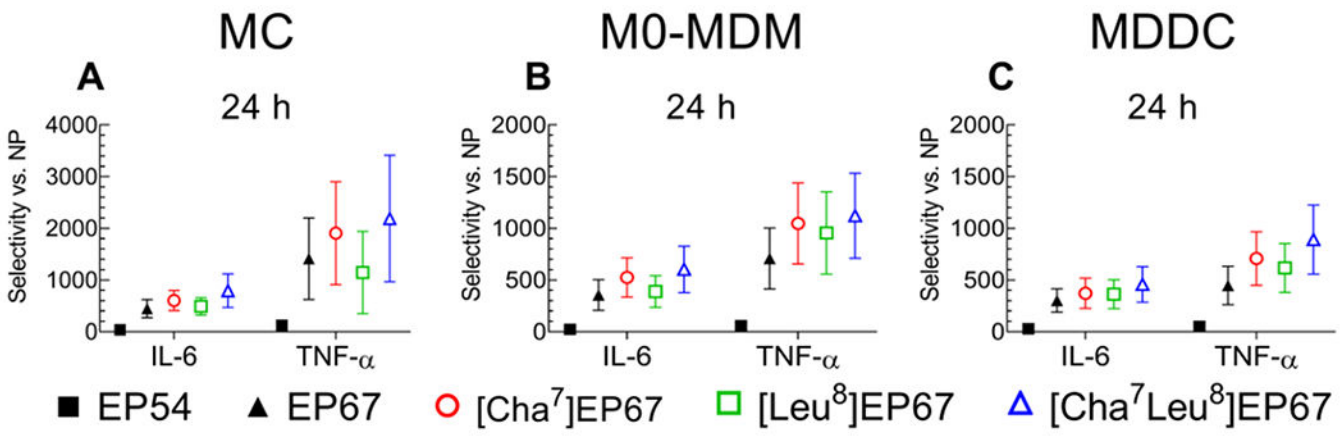

Figure 6. Comparison of selective activation of primary human mononuclear phagocytes vs. human neutrophils after treatment with human C5a desArg, EP54, EP67, or EP67 analogs for 24 h.

Average selectivities ± propagated 95% CI for stimulating the secretion of IL-6 or TNF-α from human (A) MC, (B) M0-MDM, or (C) MDDC over secretion of MPO from human neutrophils (NP) were calculated from respective EC_{50} values after treatment for 24 (Table S3).

Table 1.

Relevant sequences and molecular masses of C5a, C5a desArg, EP54, EP67, and EP67 analogs.

Peptide	IUPAC-IUB Designation	Molecular mass (g/mol)	Amino Acid Sequence
C5a	$C5a_{1-74}$	10,400 (±1,000)	---Ile^{65}Ser^{66}His^{67}Lys^{68}Asp^{69}Met^{70}Gln^{71}Leu^{72}Gly^{73}Arg^{74}
C5a desArg	$C5a_{1-73}$	10,250 (±1,000)	---Ile^{65}Ser^{66}His^{67}Lys^{68}Asp^{69}Met^{70}Gln^{71}Leu^{72}Gly^{73}
EP54	[Tyr^{65}Phe^{67}Pro^{69}Pro^{71}D-Ala^{73}]$C5a_{65-74}$	1209.6	Tyr^{01}Ser^{02}Phe^{03}Lys^{04}Pro^{05}Met^{06}Pro^{07}Leu^{08}(D-Ala)^{09}Arg^{10}
EP67	[Tyr^{65}Phe^{67}Pro^{71}Me-Leu^{72}D-Ala^{73}]$C5a_{65-74}$	1241.6	Tyr^{01}Ser^{02}Phe^{03}Lys^{04}Asp^{05}Met^{06}Pro^{07}(Me-Leu)^{08}(D-Ala)^{09}Arg^{10}
[Cha^{7}]EP67	[Tyr^{65}Phe^{67}Cha^{71}Me-Leu^{72}D-Ala^{73}]$C5a_{65-74}$	1297.7	Tyr^{01}Ser^{02}Phe^{03}Lys^{04}Asp^{05}Met^{06}**Cha**^{07}(Me-Leu)^{08}(D-Ala)^{09}Arg^{10}
[Leu^{8}]EP67	[Tyr^{65}Phe^{67}Pro^{71}Leu^{72}D-Ala^{73}]$C5a_{65-74}$	1227.6	Tyr^{01}Ser^{02}Phe^{03}Lys^{04}Asp^{05}Met^{06}Pro^{07}**Leu**^{08}(D-Ala)^{09}Arg^{10}
[Cha^{7}Leu^{8}]EP67	[Tyr^{65}Phe^{67}Cha^{71}Leu^{72}D-Ala^{73}]$C5a_{65-74}$	1283.7	Tyr^{01}Ser^{02}Phe^{03}Lys^{04}Asp^{05}Met^{06}**Cha^{07}Leu^{08}**(D-Ala)^{09}Arg^{10}

Cha = cyclohexylalanine; Me-Leu = *N*-methyl-leucine. Molecular masses of C5a and C5a desArg vary due to differences in glycosylation levels. Substitutions to amino acid residues in EP67 are highlighted in bold and underlined. C5a was not used in the current study because it is quickly converted to C5a desArg *in vivo*.

Table 2.

Summary of EP67 analog effects on EP67 potency and efficacy in primary human mononuclear phagocytes and neutrophils.

	Potency						Efficacy						Potency	Efficacy
	MC		M0-MDM		MDDC		MC		M0-MDM		MDDC		NP	NP
Peptide	IL-6	TNF-α	IL-6	TNF-α	IL-6	TNF-α	IL-6	TNF-α	IL-6	TNF-α	IL-6	TNF-α	MPO	MPO
[Cha^{7}]EP67	NC	NC	+29%	NC	NC	NC	NC	+9.5%	−9.5%	−16%	−5.2%	−16.6%	NC	−20%
[Leu^{8}]EP67	NC	NC	NC	NC	NC	NC	−9.3%	NC	NC	−23%	+41%	+45%	NC	−26%
[Cha^{7}Leu^{8}]EP67	NC	NC	+31%	NC	NC	+39%	NC	NC	−21%	−21%	−16%	−10%	NC	NC

Values calculated from Table S1 and Table S2. Cha = cyclohexylalanine, MC = human monocytes, M0-MDM = unpolarized human monocyte-derived macrophages, MDDC = human monocyte-derived dendritic cells, NP = human neutrophils, NC = no change. Increased (+) or decrease (−) %Potency = −%ΔEC_{50} or +%ΔEC_{50} vs. EP67 EC_{50} where %ΔEC_{50} = (EP67 analog EC_{50} / EP67 EC_{50}) - 1) * 100. Increased (+) or decreased (−) %Efficacy = +%ΔE_{MAX} or −%ΔE_{MAX} vs. EP67 E_{MAX} where %ΔE_{MAX} = (EP67 analog E_{MAX} / EP67 E_{MAX}) - 1) * 100%.